JOURNAL OF APPLIED ELECTROCHEMISTRY 26 (1996) 1037–1043

Anion incorporation and its effect on the dielectric constant and growth rate of zirconium oxides

M. A. ABDEL RAHIM, A. A. ABDEL RAHMAN, M. W. KHALIL

Department of Chemistry, Faculty of Science, Cairo University, Giza, Egypt

Received 23 October 1995; revised 19 January 1996

Mechanically polished zirconium electrodes were potentiodynamically polarized in phosphate buffer solutions of various pH values and in 0.5 M NaOH. The results show that the shape of the I–E curves is independent of the solution pH. At relatively low scan rates, oxygen gas evolution was observed. The oxide film thickness was calculated from the values of the charge consumed in the anodic process assuming 100% current efficiency for oxide formation below oxygen evolution (lower values for the current efficiency are assumed for potentials above oxygen evolution). Capacitance measurements, together with the calculated oxide thickness, were used to estimate values for the dielectric constant of the oxide. Two different values of the dielectric constant were obtained for the oxides formed in the range of potential below and above oxygen evolution. Also, higher dielectric constant values were obtained with increasing solution pH. Anion incorporation was assumed to increase the conductivity of the oxide films and, hence, decrease the dielectric constant. A two-layer structure is proposed for the anodically formed oxide on zirconium in aqueous solutions; an anion-free layer near the metal and an outer layer containing the incorporated anions.

1. Introduction

Anodic oxide films formed on zirconium were assumed to be homogeneous and consist mainly of ZrO_2 [1–3]. In some cases, the presence of small amounts of ZrO_3 was indicated [3]. The kinetics of anodization of zirconium depends on the nature of the electrolyte to a greater extent than the other valve metals such as Ta, Nb and Ti [4, 5]. The forming electrolyte and surface pretreatment affect both the optical constants of the oxide films on zirconium as well as the structure and the rate of oxide growth [6, 7].

The current transport in the anodization process of zirconium is assumed to be entirely due to O^{2-} migration [8, 9]. Leach *et al.* [10, 11] reported that hydrated and amorphous film forms on zirconium in the lower potential region, changing to a crystalline form at higher formation potentials, which indicates that thick zirconium oxide films are crystalline [10]. Anions from the electrolyte were found to incorporate into the zirconium oxide film, especially sulfate, carbonate and phosphate ions [11–15]. The incorporation process depends strongly on the current efficiency and the solution pH during the anodization process [16]. It was recently reported, using X-ray photoelectron spectroscopy (XPS) and Rutherford back scattering spectroscopy (RBS) [17], that the incorporated ions are closely associated in a large structure distributed regularly at the film surface. A two-layer oxide structure was proposed for films formed in H_3PO_4 [18]. The nature of the outer layer was attributed to phosphate incorporation from the electrolyte.

The aim of this paper is to investigate the effect of both anion incorporation and oxygen evolution on the kinetics of anodic oxide film growth on zirconium, and also on the electrical characteristics of this oxide.

2. Experimental details

Details of the polarization cell and measuring circuits are described elsewhere [19]. Two types of electrolyte were used: (a) buffered electrolytes (i.e., mixtures of phosphoric acid and sodium phosphates forming solutions of pH values 1.6, 2.5, 5.0, 7.0 and 9.0 and (b) unbuffered electrolytes (i.e., 0.5 M H_3PO_4, pH 0.9; 0.5 M Na_3PO_4, pH 11; and 0.5 M NaOH, pH 12).

Spectroscopically pure zirconium (Johnson Matthey, London) electrodes in the form of rods with apparent surface area 0.984 cm^2 were used. An electrode in the form of a disc with surface area 0.07 cm^2 was used for capacitance measurements. The electrode surface was mechanically polished with five grades of metallurgical papers, ending with the finest available grade (600). The electrode was then rinsed with distilled water and dried with a filter paper between the successive treatments. Following this, it was examined under magnification to ensure the absence of scratches or any similar mechanical defects. Finally, the electrode was degreased in absolute alcohol.

Mercury/mercurous sulfate/1.0 M H_2SO_4 and mercury/mercuric oxide/1.0 M NaOH electrodes were used as reference electrodes. Unless otherwise stated all potentials given refer to the normal hydrogen electrode (NHE). All electrochemical measurements were carried out in air. The temperature was adjusted to 30 ± 0.2 °C using an air thermostat.

0021-891X

3. Results and discussion

Potentiodynamic I–E measurements were performed on mechanically polished zirconium electrodes in air in phosphate solutions of varying pH 0.9–11 at a scan rate of $10\,mV\,s^{-1}$. The results are shown in Fig. 1 for which the following observations can be made:

(i) The current density rises sharply from hydrogen evolution potential to a nearly constant anodic current density region (plateau).
(ii) The current density value of the plateau increases as the solution pH increases.
(iii) At about 1.5 V, the current density starts to increase leading to another plateau of higher current density (alkaline solutions differ from the acidic ones).
(iv) At the potential value of about 1.5 V oxygen evolution was observed in all the solutions studied.

The potential value of passivation (beginning of the plateau) at each pH is more positive than the thermodynamic equilibrium potential for ZrO_2 formation [1]. This indicates that, at the plateau potential, the formation of ZrO_2 is thermodynamically possible. This potential value (ZrO_2 formation) shifts to more negative values as the pH increases in accordance with the theory [1]. The main constituents of anodic oxides are the metal ions and oxygen ions. The anodic production of zirconium oxide requires neutralizing migration of one Zr^{4+} ion from the metal at the metal/oxide interface and two O^{2-} ions from the solution at the oxide/solution interface. It appears that the migration takes place almost entirely by oxygen ions, so that the proper oxide formation occurs at the metal/oxide interface [8, 9]. Besides the metal ions and oxygen ions, foreign ions from the electrolyte may incorporate into the oxide and thus may influence the oxide film formation process. According to Leach and Pearson [11], the pick-up of anions during oxide growth depends upon the [anion/OH^-] ratio at the electrode surface. Thus, anion incorporation would be favoured at lower pH. Appreciable quantities of ions are incorporated into ZrO_2 during anodization [12, 14, 20, 21] particularly from acid solutions or solutions from which anions are strongly adsorbed into the oxide surface.

Figure 1 shows that, for a given potential, the higher the pH the higher the current density of the plateau. This can be taken as an indication that oxide films are easily formed in solutions of higher pH. The incorporation phenomenon thus decreases the concentration of O^{2-} vacancies which hinders its migration [14]. Taking into account that the anodic oxidation of zirconium has been shown to proceed almost entirely by oxygen migration, it may be expected that the incorporation of any foreign anion from the electrolyte would affect the extent of oxide growth process, in accordance with the assumption that oxide films are easily formed in solutions of higher pH, where oxygen migration is less hindered by anion incorporation.

The potentiodynamic measurements performed on zirconium in phosphate solutions (Fig. 1) were compared to a single potentiodynamic experiment in 0.5 M NaOH. The result is given in Fig. 2. Two main differences are observed with respect to Figs 1 and 2: namely, (i) the plateau current density in the anodic direction in Fig. 2 is much higher than the corresponding values of Fig. 1; and (ii) a clear anodic peak for oxygen evolution is obtained in the case of NaOH (Fig. 2), while a slight hump is observed in Fig. 1.

Anodization in NaOH solution, on the other hand, may produce a non-contaminated oxide. In this solution, anions other than OH^- are not available for incorporation, which might explain the high values of the plateau current density in that case (see

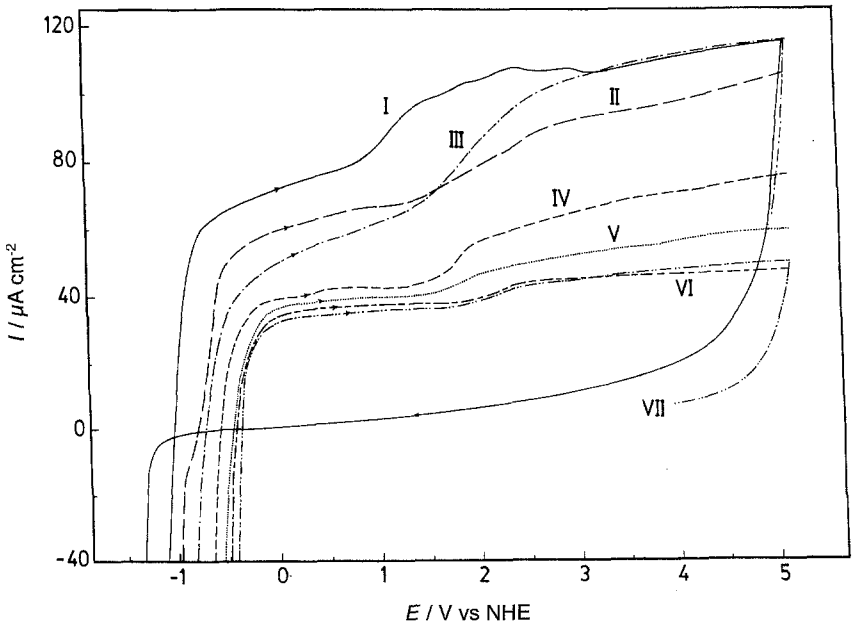

Fig. 1. Potentiodynamic polarization curves on Zr electrode in aerated phosphate buffer solutions of various pH values (scan rate: $10\,mV\,s^{-1}$): (I) 11.0, (II) 9.0, (III) 7.0, (IV) 5.0, (V) 2.5, (VI) 1.6 and (VII) 0.9.

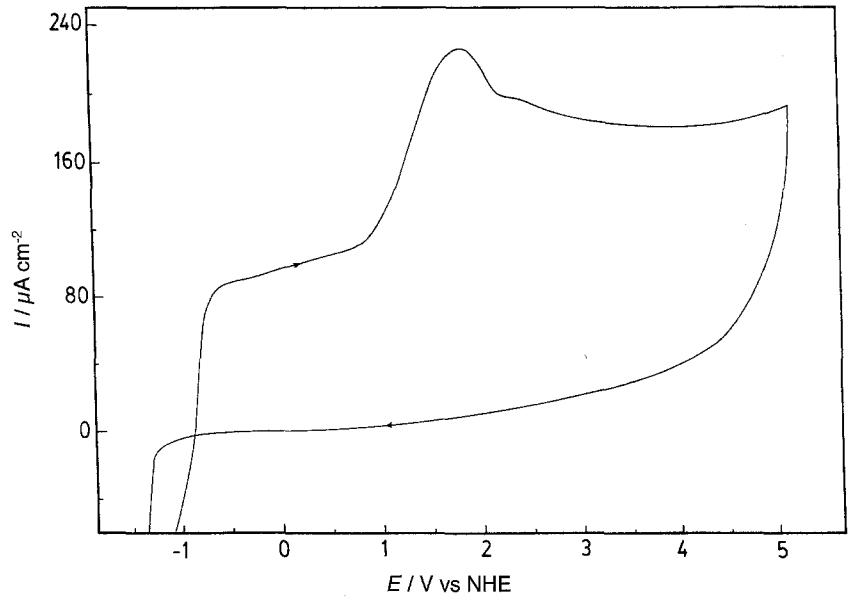

Fig. 2. Potentiodynamic polarization curve on Zr electrode in aerated 0.5 M NaOH solution (scan rate: 10 mV s^{-1}).

Fig. 2). A noncontaminated oxide was also suggested by Leach and Pearson [20] during anodization of zirconium in KOH.

Oxygen evolution was observed during the anodization of zirconium, as indicated from Figs 1 and 2, at about 1.5 V. To estimate the current efficiency for oxide film formation, some galvanostatic charging curves (potential against time at constant current density) were performed on zirconium in phosphate solutions at pH 1.6, 7.0 and 11.0 and in 0.5 M NaOH solution. Some representative results are given in Fig. 3. The results of the galvanostatic charging curves show either a bending in the E against time straight lines or a plateau in the potential range of oxygen evolution (~1.5 V). For each charging curve, the slope of the E against time straight lines was determined below and above bending or plateau (oxygen evolution). This slope, $(dE/dT)_i$, can be taken as a measure of the oxide formation rate [22]. Assuming 100% efficiency for the oxide growth below oxygen evolution [23], the efficiency above oxygen evolution can be estimated by comparing the slopes of the charging curves at each current density. Values ranging from 76.3% to 80.3% were obtained for the current efficiency in the three phosphate solutions and 59.5% in NaOH solution in the range of potential above oxygen evolution region.

It has been reported that oxides formed below and above oxygen evolution have different properties [24, 25]. The difference in properties in the case of zirconium oxides may be illustrated from the relationship shown in Fig. 4 between the anodic charge and the formation potential for zirconium oxides in four representative solutions: namely, phosphate buffers of pH 1.6, 7.0 and 11.0 and in 0.5 M NaOH. The anodic charge was calculated graphically by integrating

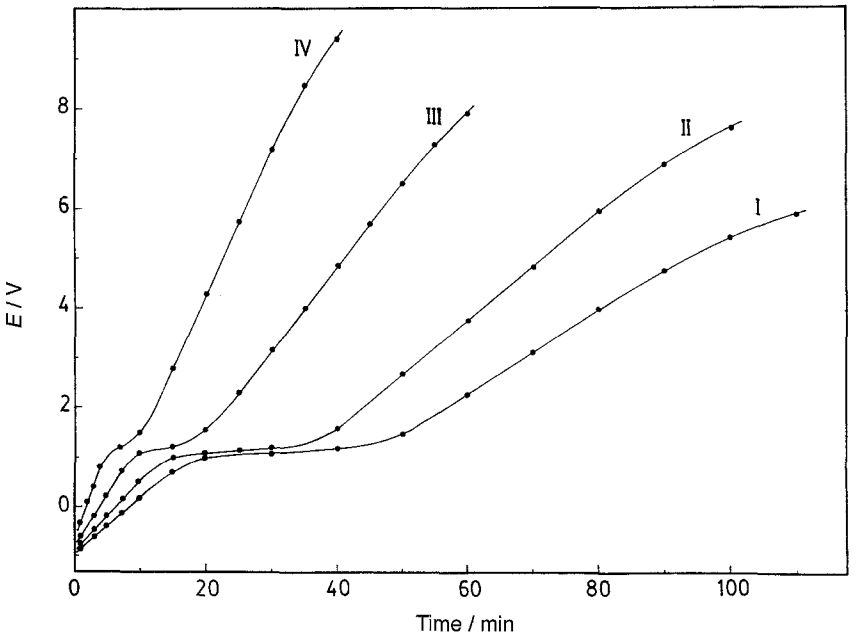

Fig. 3. Charging curves on Zr in aerated phosphate buffer solution of pH 11 at: (I) 20, (II) 30, (III) 50 and (IV) 70 μA cm^{-2}.

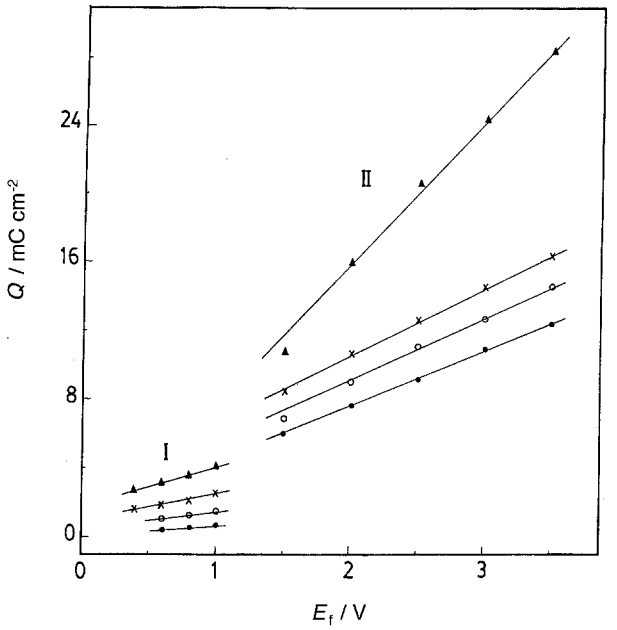

Fig. 4. Relation between the anodic charge and the formation potential in various solutions: phosphate buffer of pH: (●) 1.6, (○) 7.0 and (×) 11.0, and (▲) 0.5 M NaOH. (I) Region below oxygen evolution. (II) Region above oxygen evolution.

a set of successive potentiodynamic I–E curves carried out on Zr in the above solutions at a single scan rate of $10\,mV\,s^{-1}$. In these potentiodynamic curves, the potential was scanned from $-1.5\,V$ to $0.2\,V$ in the anodic direction and the scan was reversed in the cathodic direction to $0\,V$. At this potential, the polarization was switched off and the open-circuit capacitance of the formed oxide was immediately measured at a fixed frequency of 1.0 kHz (a conventional a.c. bridge was used [23]). The procedure was repeated reaching a different higher value of potential each time in the anodic direction, before reversing the scan and measuring the capacitance at 0 V. The values of charge obtained were determined with the assumption of 100% efficiency for the faradaic current only in the potential range below oxygen evolution (<1.5 V). In the potential range above oxygen evolution (1.5–5.0 V), it is obvious that the current efficiency for oxide film formation must be less than 100% (see Figs 1 and 2). Using the current efficiency values obtained above, the charge involved during oxide growth in the potential range above oxygen evolution was determined.

Straight line relationships with two distinct slopes were obtained in Fig. 4 for all solutions studied. Region I represents the oxide formed up to a potential value of 1.0 V (below oxygen evolution), whereas region II represents the oxide formed in the potential range from 1.5 to 3.5 V (above oxygen evolution). The lines in region II are of higher slopes than those in region I. From the slopes the anodization coefficient α (in $nm\,V^{-1}$) of oxide growth was calculated according to the equation [26]:

$$\alpha = \frac{dQ_{ox}}{dE_f}\frac{M}{nF\delta_{ox}} \qquad (1)$$

where Q_{ox} is the anodic charge and E_f is the formation potential. The quantity $M/nF\delta_{ox}$ represents the volume of oxide formed per coulomb, where M is the molecular weight of the oxide, δ_{ox} is the film density, n is the number of electrons exchanged and $F = 96\,499\,C\,mol^{-1}$. Values of $9.82 \times 10^{-5}\,cm^3\,C^{-1}$ and $5.42 \times 10^{-5}\,cm^3\,C^{-1}$ were used for amorphous and crystalline oxides, respectively.

Table 1 represents the calculated values of α, using Equation 1 at each formation potential. The values of the anodization coefficient thus obtained indicate that, for the studied solutions, oxides are formed at higher rates in the potential region above the oxygen evolution potential. This can be explained either by: (i) the catalytic effect of oxygen on the rate of oxide growth or (ii) at the potential corresponding to the oxygen evolution, small flaws are formed in the oxide through which higher rates of charge transfer can occur (see below).

Figure 4 also shows that, the rate of oxide growth increases with increasing pH with respect to the three phosphate buffer solutions, and is much higher in NaOH solution (as indicated from Table 1). The low rate of oxide growth in acidic solutions can be explained in terms of either higher oxide dissolution, or higher anion incorporation. The incorporated anions hinder O^{2-} migration through the oxide and hence reduce the rate of oxide growth. Similar behaviour was reported by Partrit *et al.* [26] who interpreted their results in terms of changes in the anodic oxide of zirconium with pH due to anion incorporation.

Leach [10] reported that change in the structure of oxide films occurs depending on the formation potential. It is probable that a hydrated and amorphous film forms in the lower potential region, changing to a more crystalline structure with increase in the formation potential [11]. Based on this argument, it can be assumed that an amorphous oxide is formed at potentials below the oxygen evolution. By increasing the formation potential, crystallization of the amorphous oxide takes place which leads to fractures and small flaws in the oxide layer. Those cause contact of the bare surface metal with the solution between the crystallites and a higher rate of charge transfer can occur, which in turn causes oxygen evolution (at about 1.5 V). Above this potential region a crystalline oxide

*Table 1. Calculated anodization coefficient α for Zr anodization in phosphate buffer solutions of pH 1.6, 7.0 and 11.0 and in 0.5 M NaOH solution (calculated from the anodic charge, Equation 1: *calculated from capacitance measurements using Equation 3)*

Anodization coefficient/nm V^{-1}		*pH of phosphate solution*			*0.5 M NaOH*
		1.6	*7.0*	*11.0*	
region I	α	0.440	0.900	1.310	2.380
	α*	0.441	0.905	1.300	2.180
	$\alpha^{\dagger}$	0.240	0.500	0.720	1.310
region II	$\alpha^{\dagger}$	1.678	1.935	2.120	4.470
	$\alpha^{\dagger}$*	1.666	1.915	2.020	4.360

α for amorphous oxides.
$\alpha^{\dagger}$ for crystalline oxides.

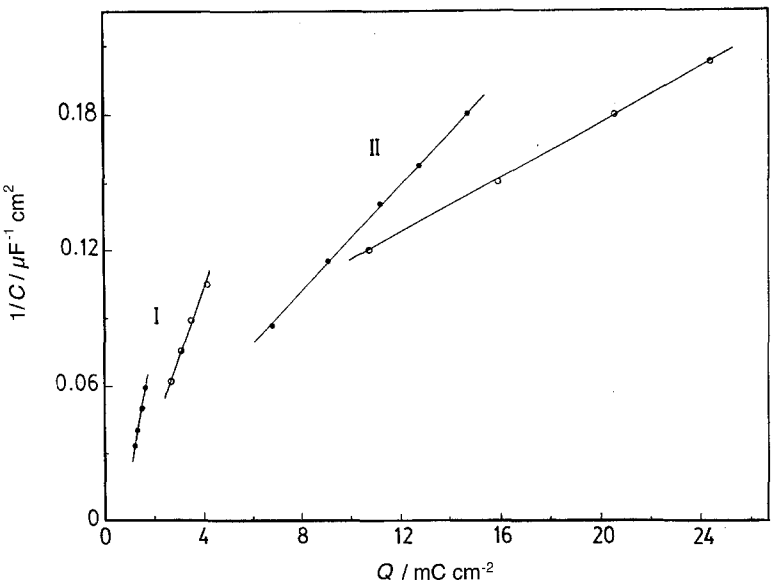

Fig. 5. Relation between the reciprocal capacitance and the anodic charge of Zr anodization in: (●) phosphate buffer solution of pH 7 and (○) 0.5 M NaOH solution. (I) Region below oxygen evolution. (II) Region above oxygen evolution.

may be formed. In this case two different dielectric constant values are to be expected, one value for oxides formed in the range of potential below oxygen evolution and the other in the range of potential above oxygen evolution potential. Another proposed cause for oxygen evolution during the anodization of zirconium was given in the literature as the effect of intermetallic precipitates from zirconium impurities [7, 18].

The following equation relates the reciprocal capacitance, $1/C$, of the oxide to the anodic charge, Q_{ox}, consumed in its formation [27]:

$$\frac{1}{C} = \frac{d_o}{DD_0 r} + \frac{Q_{ox}M}{nF\delta_{ox}DD_0 r^2} \qquad (2)$$

where d_0 is the prepolarization thickness, D is the dielectric constant of the oxide, $D_0 = 8.85 \times 10^{-14}$ F cm^{-1} is the dielectric constant of the vacuum [28] and r is the roughness factor (a value of 1.2 was used [27]). From this equation a linear relation between $1/C$ and the accumulated charge Q_{ox} (as a function of thickness d) is expected. Figure 5 shows this relationship for the oxides formed at different formation potentials, and the experimental values of the anodic charge, Q_{ox}, for the oxides formed in some representative solutions. A straight line relation of two slopes was also obtained in all solutions, one for the oxides formed in the range of potential below the oxygen evolution (region I) and another of much lower slope for oxides formed in the range of potential above the oxygen evolution (region II). The extrapolation of the straight line of region I to $1/C = 0$ yields, for all solutions, a charge $Q^{o}_{ox} = 0.725$ mC cm^{-2}, which corresponds to a thickness of 0.60 nm or 0.34 nm for the initial oxide film d_0 for the amorphous and crystalline oxides, respectively. Those comparatively low values of d_0 may result from dissolution of the oxide during hydrogen evolution at the beginning of polarization. Higher values of d_0 at zirconium were reported [7, 27]. From the slopes of the straight lines in Fig. 5 the dielectric constant of the oxide was calculated. Table 2 shows values of the dielectric constant for amorphous and crystalline ZrO_2 in all solutions studied in the range of potential below I and above II oxygen evolution. It is observed that the dielectric constant value in region II is much higher than that obtained in region I. These large variations in the value of dielectric constant were always obtained independent of the calculation method used. That is, the proposed value of the density of the oxide (3.25 g cm^{-3} for amorphous and 5.89 g cm^{-3} for crystalline oxide) does not influence the general trend in the variation of dielectric constant. It was also found that the value of the dielectric constant increases with increasing pH for the three buffered phosphate solutions and more so for NaOH solution (Table 2). This is to be expected, as the characteristics of the oxide film are a function of the electrolyte composition in which they are formed [18, 26, 28]. But the increase in the dielectric constant with increasing pH can be interpreted in terms of anion incorporation. Anion incorporation is assumed to increase the conductivity of the oxide films and, hence, decreases the dielectric constant. A similar conclusion has been drawn by Di Quarto *et al.* [29] and Randall *et al.* [30]. For this reason the lower values of the dielectric constant measured in the acidic solutions may be attributed to the high degree of anion incorporation at low pH. The highest value of the

Table 2. Estimated dielectric constant values for Zr oxides formed anodically in phosphate buffer solutions and in 0.5 M NaOH solution

Dielectric constant		*pH of phosphate solution*			*0.5 M NaOH*
		1.6	*7.0*	*11.0*	
Region I	D	19.2	27.7	30.8	38.5
	$D^{\dagger}$	10.6	15.3	17.0	21.3
Region II	$D^{\dagger}$	42.5	55.8	70.2	107.7

D for amorphous oxides.
$D^{\dagger}$ for crystalline oxides.

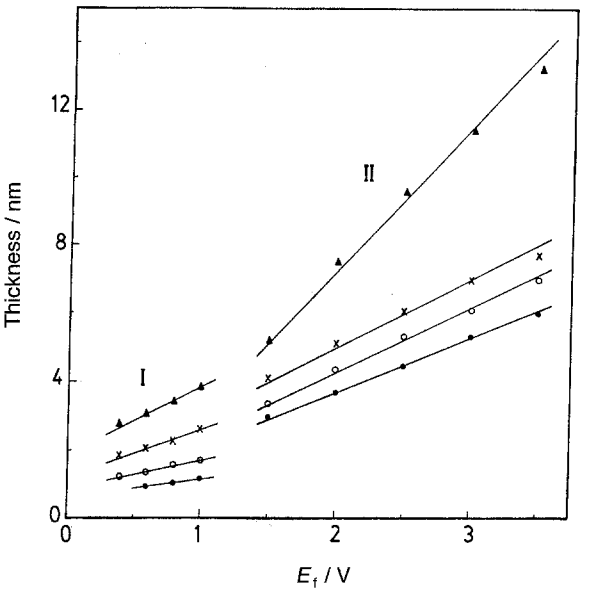

Fig. 6. Relation between the total oxide film thickness (d) and the formation potential (E_f) of Zr anodization in phosphate buffer solutions of pH: (●) 1.6, (○) 7.0 and (×) 11.0 and in (▲) 0.5 M NaOH. (I) Region below oxygen evolution. (II) Region above oxygen evolution.

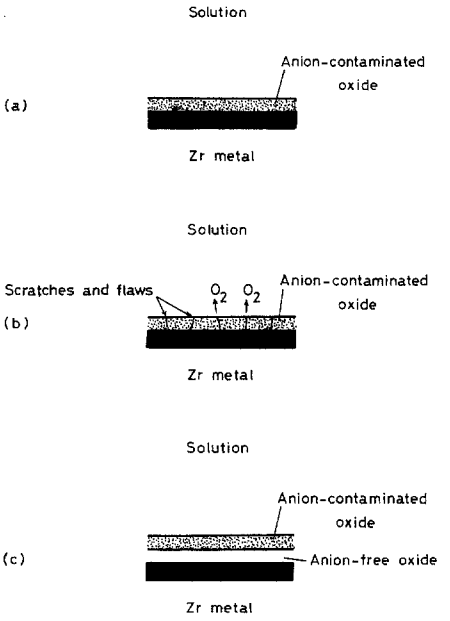

Fig. 7. Schematic representation of the process of anodic oxide growth on Zr in aqueous solutions. (a) Below oxygen evolution. (b) Crack formation at oxygen evolution. (c) Crack repair above oxygen evolution.

dielectric constant was obtained in NaOH solution where no anion incorporation is expected.

Using the value of $d_o = 0.60$ nm for amorphous oxide or $d_o = 0.34$ nm for crystalline, it was possible to calculate the total oxide thickness d [27]. A plot of the total thickness against formation potential (Fig. 6) yields a straight line relation of two slopes corresponding to the two regions. Figure 6 shows that the acidic solutions are associated with low oxide thickness and *vice versa*.

The oxide growth rate can also be estimated from the capacitance values, C, measured at each formation potential, E_f, according to the following equation [27]:

$$\frac{1}{C} = \frac{\alpha}{DD_o r}(E_f - E_{ox}) \qquad (3)$$

where α is the anodization coefficient, D is the dielectric constant of the oxide, D_o is the dielectric constant of vacuum, r is the roughness factor and E_{ox} is the potential of the beginning of oxide formation. The values of α are in excellent agreement with those obtained using the charge involved during oxide growth using Equation 1 (see Table 1).

4. Conclusion

It is proposed that at the beginning of anodization an amorphous ZrO_2 is formed. Increasing the anodization potential increases the thickness of the oxide by the anodic oxidation of zirconium almost entirely through O^{2-} migration. At the same time, the incorporation of foreign anions from the electrolyte occurs and affects the extent of oxide growth and, accordingly, limits the oxide thickness. Consequently, at low formation potentials an anion-contaminated oxide is formed ((a) in Fig. 7). By increasing the anodization potential and in the potential range just below oxygen evolution, crystallization of the amorphous oxide takes place. The crystallization process leads to the formation of microfractures that, in turn, cause a temporary breakdown of the oxide, which results in increasing metal–solution contact between the crystallites. Higher rates of charge transfer results in increasing evolution of oxygen gas ((b) in Fig. 7). The fractures in the oxide are then repaired as the potential increases and the presence of oxygen catalyses the oxidation process. Thus, above the oxygen evolution, a higher rate of oxide growth is achieved which leads to a noncontaminated oxide near the metal, ((c) in Fig. 7). Therefore, a two-layer structure is proposed: an anion-free oxide layer near the metal, and an outer layer containing the incorporated species. This two-layer structure is consistent with the duplex nature of oxide films on zirconium and other valve metals [6, 31–33].

With regard to the anodization of zirconium in NaOH solution, in which no anion incorporation occurs, a duplex structure is also expected as indicated by the two straight lines obtained in Figs 4 and 6. The duplex structure is formed because of the difference in the oxide hydration. A hydrated oxide is obtained at the oxide/solution interface as an outer oxide film, and an anhydrous inner oxide film is also formed [34].

References

[1] M. Pourbaix, 'Atlas of Electrochemical Equilibria in Aqueous Solutions', Pergamon Press, London (1966) p. 223.
[2] T. P. Bondareva and V. M. Novakovskii, *Zashch. Metal.* **6** (1970) 207.
[3] F. F. Faizullin and N. D. Mazurenko, *Issled. Elektrokhim., Magnetokhim. Metod. Anal.*, no. 2 (1969) 136.
[4] G. Kalyani, A. Pansa Reddy and K. S. Sastry, *Z. Phys. Chem.* **269** (1988) 201.
[5] G. Kalyani and K. S. Sastry, *Bull. Electrochem.* **7** (1991) 22.
[6] E. M. Patrito and V. A. Macagno, *J. Electroanal. Chem.* **371** (1994) 59.

[7] *Idem, J. Electrochem. Soc.* **140** (1993) 1576.
[8] J. L. Whitton, *J. Electrochem. Soc.* **115** (1968) 59.
[9] J. A. Davies, B. Komeij, T. P. S. Pringle and F. Browm, *ibid.* **112** (1965) 675.
[10] J. S. L. Leach and B. R. Pearson, *Corros. Sci.* **28** (1988) 43.
[11] J. S. L. Leach and B. R. Pearson, *Electrochim. Acta* **29** (1984) 1263.
[12] J. S. L. Leach and C. N. Panagopoulos, *ibid.* **31** (1986) 1577.
[13] J. A. Bardwell and M. C. H. McKubre, *ibid.* **36** (1991) 647.
[14] J. S. L. Leach and B. R. Pearson, *ibid.* **29** (1984) 1271.
[15] J. C. Banter, *J. Electrochem. Soc.* **114** (1967) 508.
[16] J. S. L. Leach, C. N. Panagopoulos and B. R. Pearson, The Electrochemical Society Extended Abstracts, Minneapolis, MN, 10–15 May (1981), Abstract 28, p. 91; J. S. L. Leach and C. Panagopoulos, 32nd ISE Meeting, Cavat, September (1981), Extended Abstracts, vol. II p. 1002.
[17] N. Magnussen, L. Quinones, D. L. Cocke, E. A. Schweikert, B. K. Patnaik, C. V. Barros Leite and G. B. Baptista, *Thin Solid Films* **167** (1988) 245.
[18] E. M. Patrito and V. A. Macagno, *J. Electroanal. Chem.* **375** (1994) 203.
[19] M. W. Khalil, M. A. Abdel Rahim, *Mat-wiss.u. Werkstofftech.* **22** (1991) 260.
[20] J. S. L. Leach and B. R. Pearson, Proceedings of the 7th International Congress on Metallic Corrosion, Rio de Janeiro, ABRACO (1978) p. 151.
[21] G. T. Rogers, P. H. G. Draper and S. S. Wood, *Electrochim. Acta* **13** (1968) 251.
[22] I. A. Ammar, S. Darwish and M. W. Khalil, *Z. Werkst.tech.* **12** (1981) 421.
[23] S. Darwish, M. W. Khalil, M. A. Abdel Rahim and I. A. Ammar, *Mat-wiss.u. Werkstofftech.* **20** (1989) 299.
[24] T. Shibata and M. A. M. Ameer, *Denki Kagaku* **60** (1992) 494.
[25] N. D. Mazurenko and F. F. Faizulline, *Sb. Aspir. ab., Kazan. Gos. Univ., Khim., Geogr., Geol.* (1970) 16–19.
[26] E. M. Patrito, R., Torresi, E. P. M. Leiva and V. A. Macagno, *J. Electrochem. Soc.* **137** (1990) 524.
[27] P. Meisterjahn, H. W., Hoppe and J. W. Schultze, *J. Electroanal. Chem. Interfacial Electrochem.* **217** (1987) 159.
[28] L. Young, *Proc. R. Soc. Lond. A* **244** (1958) 41.
[29] F. Di Quarto, A. Di Paola and C. Sunseri, *J. Electrochem. Soc.* **127** (1980) 1016.
[30] J. J. Randall, W. J. Bernard and R. R. Wilkinson, *Electrochim. Acta* **10** (1965) 183.
[31] M. S. El-Basiouny, A. A. Mazhar, F. El-Taib and M. A. Ameer, *J. Electroanal. Chem. Interfacial Electrochem.* **147** (1983) 181.
[32] H. Takahashi, K. Fujimoto and M. Nagashama, *J. Electrochem. Soc.* **135** (1988) 1349.
[33] I. Montero, J. M. Albella and J. M. Martinez-Duart, *ibid.* **132** (1985) 976.
[34] A. Clearfield, *Inorg. Chem.* **3** (1964) 146.